Research Article | Vol. 25, No. 22 | 30 Oct 2017 | OPTICS EXPRESS 27818
Optics EXPRESS

# Linear Cherenkov radiation in ferroelectric domain walls

**JI YANG,[1,2] XIAOHUI ZHAO,[3] HAIGANG LIU,[1,2] AND XIANFENG CHEN[1,2,*]**

[1]*State Key Laboratory of Advanced Optical Communication Systems and Networks, School of Physics and Astronomy, Shanghai Jiao Tong University, Shanghai 200240, China*
[2]*Key Laboratory for Laser plasma (Ministry of Education), Collaborative Innovation Center of IFSA (CICIFSA), Shanghai Jiao Tong University, Shanghai 200240, China*
[3]*Shanghai Institute of Laser Plasma, Shanghai 201800, China*
**xfchen@sjtu.edu.cn*

**Abstract:** Nonlinear Cherenkov radiation plays an important role in detecting the internal structure of the ferroelectric crystal. However, linear Cherenkov radiation in the ferroelectric crystal was not observed before. Based on mirror symmetry reduction at the domain walls, we theoretically predicted that the linear Cherenkov radiation could be generated in periodically poled ferroelectric crystals according to the coupled wave equation. Then, we experimentally demonstrated the generation of such Cherenkov radiation in domain walls. Compared with the domain region, new nonzero elements $\chi_{13}$, $\chi_{23}$, $\chi_{31}$ and $\chi_{32}$ appear in the linear susceptibility tensor. The experimental results are consistent with our theoretical prediction.



**OCIS codes:** (240.0240) Optics at surfaces; (160.4330) Nonlinear optical materials.

## References and links

1. P. A. Cherenkov, "Visible emission of clean liquids by action of γ radiation," Dokl. Akad. Nauk SSSR **2**, 451 (1934).
2. A. Zembrod, H. Puell, and J. Giordmaine, "Surface radiation from non-linear optical polarisation," Opto-electronics **1**(1), 64–66 (1969).
3. H. Ren, X. Deng, Y. Zheng, N. An, and X. Chen, "Enhanced nonlinear Cherenkov radiation on the crystal boundary," Opt. Lett. **38**(11), 1993–1995 (2013).
4. P. Molina, M. O. Ramírez, B. J. García, and L. E. Bausá, "Directional dependence of the second harmonic response in two-dimensional nonlinear photonic crystals," Appl. Phys. Lett. **96**(26), 261111 (2010).
5. S. M. Saltiel, D. N. Neshev, R. Fischer, W. Krolikowski, A. Arie, and Y. S. Kivshar, "Generation of secondharmonic bessel beams by transverse phase-matching in annular periodically poled structures," Jpn. J. Appl. Phys. **47** (8S1), 6777– 6783 (2008).
6. W. Wang, Y. Sheng, Y. Kong, A. Arie, and W. Krolikowski, "Multiple Čerenkov second-harmonic waves in a two-dimensional nonlinear photonic structure," Opt. Lett. **35**(22), 3790–3792 (2010).
7. Y. Sheng, D. L. Ma, and A. Krolikowski, "Randomized nonlinear photonic crystal for broadband optical frequency conversion," J. Phys. At. Mol. Opt. Phys. **46**(21), 215401 (2013).
8. S. J. Holmgren, C. Canalias, and V. Pasiskevicius, "Ultrashort single-shot pulse characterization with high spatial resolution using localized nonlinearities in ferroelectric domain walls," Opt. Lett. **32**(11), 1545–1547 (2007).
9. Y. Sheng, A. Best, H. J. Butt, W. Krolikowski, A. Arie, and K. Koynov, "Three-dimensional ferroelectric domain visualization by Čerenkov-type second harmonic generation," Opt. Express **18**(16), 16539–16545 (2010).
10. C. Chen, J. Lu, Y. Liu, X. Hu, L. Zhao, Y. Zhang, G. Zhao, Y. Yuan, and S. Zhu, "Cerenkov third-harmonic generation via cascaded $\chi^{(2)}$ processes in a periodic-poled $LiTaO_3$ waveguide," Opt. Lett. **36**(7), 1227–1229 (2011).
11. Y. Zhang, Z. D. Gao, Z. Qi, S. N. Zhu, and N. B. Ming, "Nonlinear Cerenkov radiation in nonlinear photonic crystal waveguides," Phys. Rev. Lett. **100**(16), 163904 (2008).
12. N. An, Y. Zheng, H. Ren, X. Zhao, X. Deng, and X. Chen, "Normal, degenerated, and anomalous-dispersion-like Cerenkov sum-frequency generation in one nonlinear medium," Photonics Res. **3**(4), 106–109 (2015).
13. A. S. Aleksandrovsky, A. M. Vyunishev, A. I. Zaitsev, A. A. Ikonnikov, and G. I. Pospelov, "Ultrashort pulses characterization by nonlinear diffraction from virtual beam," Appl. Phys. Lett. **98**(6), 061104 (2011).
14. A. Fragemann, V. Pasiskevicius, and F. Laurell, "Second-order nonlinearities in the domain walls of periodically poled $KTiOPO_4$," Appl. Phys. Lett. **85**(3), 375–377 (2004).
15. G. Catalan, J. Seidel, R. Ramesh, and J. F. Scott, "Domain wall nanoelectronics," Rev. Mod. Phys. **84**(1), 119–156 (2012).

#306380 https://doi.org/10.1364/OE.25.027818
Journal © 2017 Received 5 Sep 2017; revised 14 Oct 2017; accepted 22 Oct 2017; published 26 Oct 2017

Optics EXPRESS

16. X. Deng, H. Ren, H. Lao, and X. Chen, "Research on Cherenkov second-harmonic generation in periodically poled lithium niobate by femtosecond pulses," J. Opt. Soc. Am. B **27**(7), 1475–1480 (2010).
17. H. Ren, X. Deng, Y. Zheng, N. An, and X. Chen, "Nonlinear Cherenkov radiation in an anomalous dispersive medium," Phys. Rev. Lett. **108**(22), 223901 (2012).
18. B. Liu, Y. Zheng, X. Zhao, H. Liu, and X. Chen, "Probe of symmetry reduction at domain walls by nonlinear Cherenkov measurement," Opt. Express **24**(26), 29459–29464 (2016).
19. X. Deng and X. Chen, "Domain wall characterization in ferroelectrics by using localized nonlinearities," Opt. Express **18**(15), 15597–15602 (2010).
20. D. A. Scrymgeour, V. Gopalan, A. Itagi, A. Saxena, and P. J. Swart, "Phenomenological theory of a single domain wall in uniaxial trigonal ferroelectrics: Lithium niobate and lithium tantalate," Phys. Rev. B **71**(18), 184110 (2005).

## 1. Introduction

In particle physics, the coherent electromagnetic wave can be emitted when the velocity of a charged particle exceeds the light velocity in a non-vacuum transparent medium, known as the traditional Cherenkov radiation (CR) [1]. Not only in particle physics, the phenomenon of such CR has been investigated in the field of the nonlinear optics, which terms as the nonlinear Cherenkov radiation (NCR) [2]. Compared with the CR process of accelerated charged particles, the radiation source of NCR is not a point particle, but a spatially extended collection of dipoles driven by the incident light field, that is the polarization $\vec{P}$. In recent years, NCR has attracted considerable interest [3] and it has been observed in a variety of nonlinear photonic crystals (NPCs), such as one-dimensional periodical, square, hexagonal lattices, annular, periodical or even random structures [4–7]. So far, it has been widely applied to domain walls imaging [8, 9], high-order harmonic generation [10, 11], sum-frequency generation [12], ultrashort pulse characterization [13], and so on. In previous study on NCR, domain walls as the ultrathin planar material in periodically poled ferroelectrics generate stronger NCR than single-domain area [14]. The mechanism of enhanced process in domain walls may be attributed to the new enhanced susceptibility tensor elements owing to the lattice distortion or the localized internal electrical field at domain walls [15, 16]. In addition, some specific properties, such as conductive and photovoltaic characteristics also have been demonstrated on domain walls [15, 17]. In the previous research, the break of mirror symmetrical property has been verified in the domain walls [18].

In this paper, based on the mirror symmetry reduction of domain walls, we theoretically predict that the linear Cherenkov radiation (LCR) could be generated in ferroelectric crystal according to the coupled wave equation. Then, we experimentally demonstrate the generation of such LCR in the domain walls. As far as we know, this is the first time to observe the LCR in the domain walls structure. According to our analysis, the modulation of the domain walls to the LCR is similar to the nonlinear process. Comparing with the domain region, new nonzero elements $\chi_{13}$, $\chi_{23}$, $\chi_{31}$ and $\chi_{32}$ appear in the linear susceptibility tensor of domain walls, which is consistent with theoretical prediction.

## 2. Theoretical prediction

For linear processes in bulk $LiNbO_3$, the linear polarization wave $P$ can be expressed by the incident wave $E$ and the linear susceptibility $\chi^{(1)}$ in the form of

$$\begin{pmatrix} P_x \\ P_y \\ P_z \end{pmatrix} = \varepsilon_0 \begin{pmatrix} \chi_{11} & 0 & \underline{0} \\ 0 & \chi_{22} & \underline{0} \\ \underline{0} & \underline{0} & \chi_{33} \end{pmatrix} \begin{pmatrix} E_x \\ E_y \\ E_z \end{pmatrix}, \tag{1}$$

where $\varepsilon_0$ is the vacuum permittivity.

In Eq. (1), the underlined zero elements are determined by the mirror inversion symmetry with respect to y-z plane. However, in Ref [18], we have demonstrated that the mirror symmetrical property in the domain walls were broken. Hence, the underlined elements are not equal to 0. In such situation, without loss of generality, we assume that $\chi_{13} \neq 0$. Supposing the incident light is e-polarized Gaussian wave $E_z$ with width $a$, and the o-polarized light can be emitted and expressed as $E'_x$. The coupling between the two beams is governed by the element $\chi_{13}$, which spatially depends on *x*. As shown in Fig. 1(a), $g(x)$ is the periodic function representing the distributed function of $\chi_{13}$, $g(x)$ is equal to 0 except in domain walls, $\Lambda$ is the poling period and $d$ is the width of the domain wall.

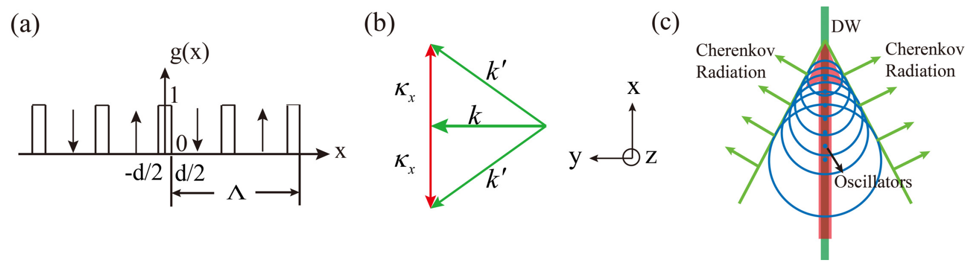


Fig. 1. (a) The distributed function of $\chi_{13}$ modulated by domain walls. (b) Phasing matching diagram of $k$, $k'$ and $\kappa_x$. (c) Diagram of Cherenkov radiation.

The $x$ component of displacement vector $D'$ satisfies

$$D_x{}' = \varepsilon_0 E_x{}' + P_x = \varepsilon_0 E_x{}' + \varepsilon_0 \left[ \chi_{11} E_x{}' + \chi_{13} g(x) E_z \right]. \tag{2}$$

In such process, the relevant amplitude of emitting wave is written as $E'_x = A'(x,y)e^{-i(k'y-\omega t)}$.

Under the slowly varying envelop approximation, the evolution of the amplitude of o-polarized emitting wave in the crystal can be written as:

$$\left( \frac{\partial}{\partial y} + \frac{i}{2k'} \frac{\partial^2}{\partial^2 x} \right) A'(x,y) = -i \frac{\mu_0 \varepsilon_0 \omega^2}{2k'} \chi_{13} g(x) A e^{-i(k'-k)y} F(x), \tag{3}$$

where $F(x) = exp(-x^2/a^2)$ is the transverse distribution of incident Gaussian beam, $A$ and $A'(x,y)$ denote the complex amplitudes of the incident wave and emitted wave, respectively. By using the method of Fourier transform, we solve the coupling wave equation, considering the intensity $S'(\kappa_x, y) = \left| A'(\kappa_x, y) \right|^2$ of emitted wave, we obtain

$$\begin{aligned} S'(\kappa_x, y) = & \left( y \chi_{13} A \cdot \sqrt{\pi} \cdot \frac{\mu_0 \varepsilon_0 \omega^2}{2k'} \right)^2 \cdot \left\{ \sin c \left[ \left( \Delta k - \frac{\kappa_x^2}{2k'} \right) \frac{y}{2} \right] \right\}^2 \\ & \cdot \left\{ a \sum_{m \neq 0} g_n e^{-\frac{a^2 (mG_0 - \kappa_x)^2}{4}} + \frac{a e^{-\frac{a^2 \kappa_x^2}{4}}}{2} \left[ erf\left( \frac{d - ia^2 \kappa_x}{2a} \right) + erf\left( \frac{d + ia^2 \kappa_x}{2a} \right) \right] \right\}^2, \end{aligned} \tag{4}$$

where $\kappa_x = k' sin\gamma$ is the transverse wave vector of the emitting wave as shown in Fig. 1(b), $\Delta k = k' - k$ is the phase mismatch between incident and emitting waves, $\gamma$ is the radiation angle, and $erf(x)$ is the Gauss error function.

Optics EXPRESS

Equation (4) indicates that, the *sinc* function is maximum when $\Delta k - k_x^2 / 2k' = 0$. By using the approximate expression $(1 - k_x / k')^{1/2} \approx 1 - k_x / 2k'$, the solution of $\Delta k - k_x^2 / 2k' = 0$ can evolve into $k'^2 - k^2 = k_x^2$. From the geometrical relationship, the relation is deduced to $cos\theta = k / k'$, which is exactly the longitudinal phase-matching condition of Cherenkov radiation process as shown in Fig. 1(b). Therefore, such discontinuous distribution of non-diagonal elements of linear susceptibility tensor leads to the LCR. That means, when a polarized light propagates in the crystal, it can stimulate the linear polarization wave, resulting in radiating the light with different polarization state in the Cherenkov direction, as shown in Fig. 1(c).

According to Eq. (4), we simulate the intensity distribution of the emitted wave in PPLN, as shown in Fig. 2(a). The internal radiation angle of the efficient emitting light is $17^\circ$. The emitted light also has a component along $y$ direction, the form of expression $E_y'$ is similar to $E_x'$ which is related to $\chi_{23}$. In Fig. 2(b), we show the relationship between the intensity of LCR and the thickness of domain wall. According to the simulation, the corresponding domain wall thickness of the maximum LCR intensity is about 0.4 $\mu m$. However, the width of ferroelectric domain wall is only several lattice units [19, 20]. Hence the LCR is relatively weak in the actual experiment.

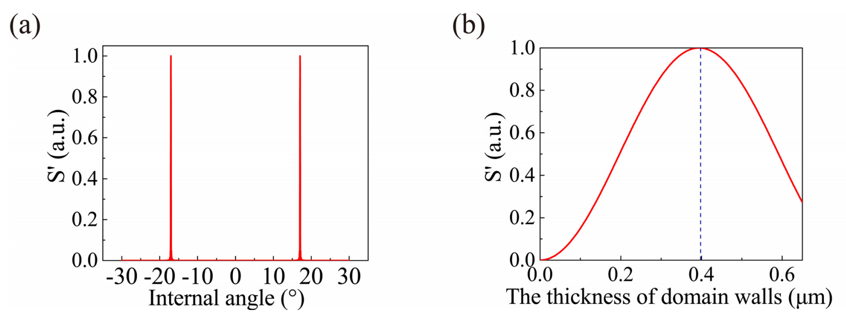


Fig. 2. (a) Angular distribution of emitting light for the incident wavelength of 532 nm. (b) The relationship between the intensity of LCR and the thickness of domain wall ( $a = 50\mu m$ ).

## 3. Experimental results and discussion

In our experiment, a mode-locked Nd:YAG laser (532 nm) producing about 10.5-ns pulses with 5 mJ per pulse energy at a repetition of 1 kHz was used as the source. We used the z-cut (z axis is the polar axis of the crystal) periodically poled 5 mol% MgO:$LiNbO_3$ of the size of $20 \times 4 \times 1$ mm$^3$ (x × y × z). The domain walls of PPLN were parallel to the y-z plane. The poling period Λ was 30 μm and the duty ratio was 1:1. The incident light was loosely focused into the sample by a 100-mm focal lens. The focus size of the incident light is about 100 micrometers. A polarizer was utilized to check the polarization of the emitted light.

The e-polarized laser beam, whose polarization is along z-axis, propagates along y-axis of the PPLN. The schematic of the experimental setup to realize the LCR in PPLN is shown in Fig. 3(a). According to the Sellmeier equation, the refractive index of the o-polarized incident light ( $n_o = 2.33$ ) is larger than the e-polarized light ( $n_e = 2.23$ ). It means that the polarization wave excited by the incident light propagates faster than the o-polarized light. Therefore, if the LCR can be generated, the o-polarized beam would be observed at the linear Cherenkov angle $\gamma = \arccos(k_1 / k_2)$. The experimental result is shown in Fig. 1(b). An e-polarized spot and a pair of o-polarized Cherenkov spots located in the center and two sides on the screen, respectively. The angle between LCR spot and incident light is about $41.7^\circ$, it can be

Optics EXPRESS

converted into internal angle $16.6^{\circ}$, which is in well agreement with the calculated internal Cherenkov angle $17^{\circ}$ in PPLN.

Considering the oblique beam of the generating LCR spots, the electric component contains $E_x$ and $E_y$. According to Eq. (1), we can obtain $\chi_{13} \neq 0$ and $\chi_{23} \neq 0$ in the $\chi^{(1)}$ tensor of domain walls, which is consistent with our previous prediction about $\chi_{13}$ in the part of theoretical prediction. By tuning the incident angle $\beta$, o-polarized wave could be observed at different radiation angles. Figure 3(c) shows the relationship between external LCR angle and the incident angle, in which the experimental results are in well agreement with the theoretical calculation.

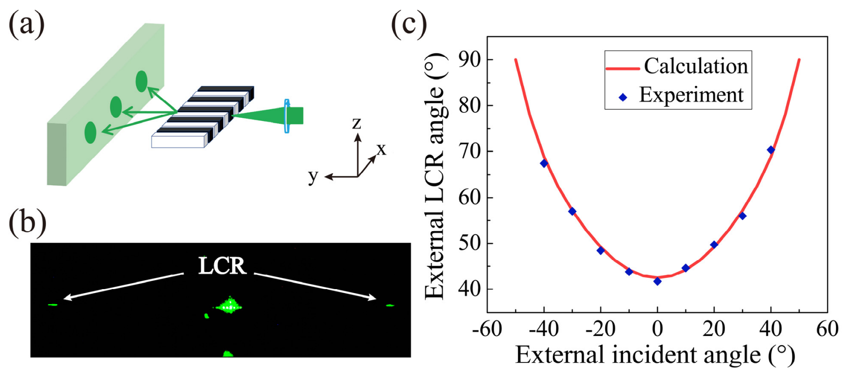


Fig. 3. (a) Schematic of the experimental setup. (b) LCR on the screen with the e-polarized incidence. (c) The relationship between external LCR angle and external incident angle. Theoretical calculation (the solid line) and experimental results (symbols) are in well agreement with each other.

The polarization state of incident light is changed to be o-polarized. When the incident light is perpendicular to the domain wall ($k_o > k_e$), the LCR cannot be generated. However, due to the modulation effect of the domain wall, the phase velocity of polarization wave can be tuned from the velocity of incident light to infinity by changing the incident angle $\beta$ with respect to the domain wall [18, 20]. In this situation, the wave vector of linear polarization wave is $k_p = kcos\beta$ along the domain wall direction. The phase velocity is $v_p = v / cos\beta$ and the LCR angle $\gamma$ satisfies:

$$\cos\gamma = k_p / k' = k\cos\beta / k' = n\cos\beta / n', \tag{5}$$

where $k'$ is the wave vector of LCR, $n$ and $n'$ denote the refractive index of the incident and emitted light, respectively.

The recorded patterns with different external incident angles $0^{\circ}$, $15^{\circ}$, $42.2^{\circ}$ and $48.9^{\circ}$ are presented in Fig. 4(a). The relationship between external incident angle $\alpha$ and internal angle $\beta$ is $\sin\alpha = n_o \sin\beta$. There are three stages with different $\beta$: I $0^{\circ} \leq \beta \leq cos^{-1}(n' / n)$; II $\beta = cos^{-1}(n' / n)$ and III $cos^{-1}(n' / n) \leq \beta \leq 90^{\circ}$. In stage I, the phase velocity of linear polarization wave does not exceed the e-polarized wave. The LCR condition cannot be satisfied and the phase-matching geometry is shown in the left of Fig. 4(b). In this situation, the LCR generated by two subcarriers on the domain wall cannot constructively interfere, hence, the LCR cannot be observed. The corresponding experimental results are shown in the first and second row of Fig. 4(a). In stage II, the phase-matching condition shows in the middle of Fig. 4(b). In this stage, the incident angle just reaches the critical angle ($\beta = 16.8^{\circ}$)

Optics EXPRESS

of the LCR. Therefore, only a collinear e-polarized LCR spot, which terms as the degenerate LCR, is observed in the experiment, as shown in the third row of Fig. 4(a). While in stage III, the phase velocity of linear polarization wave exceed the e-polarized wave and the phase-matching condition shows in the right of Fig. 4(b). Therefore, the generated e-polarized LCR splits into two spots. The experimental result of the case of external incident angle $\alpha = 48.9^{\circ}$ is illustrated in the last row of Fig. 4(a). The relationship between external LCR angle and external incident angle is shown in Fig. 4(c), in which the experimental measurement is consistent with the theoretical calculation. In this case, the symmetrical Cherenkov spots are e-polarized. According to Eq. (1), we can conclude that $\chi_{31} \neq 0$ and $\chi_{32} \neq 0$. But $\chi_{12}$ and $\chi_{21}$ cannot be determined in our experiment.

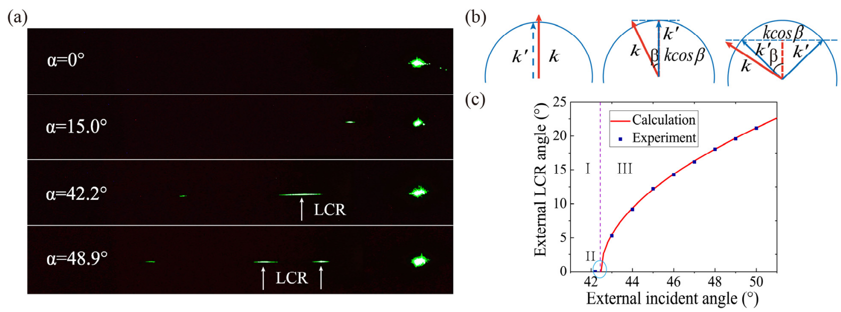


Fig. 4. (a) The experimental results of LCR with varying incident angles. (b) The phase-matching geometry of different stage. (c) The relationship between external CR angle $\theta$ and external incident angle.

Not limited in PPLN crystal, such LCR could also be observed in other optical interface. In our experiment, the conversion efficiency of the LCR is relatively weak. It attribute to the thickness of domain walls, which only several lattice units. One possible method to increase such LCR intensity is to artificially fabricate a similar domain walls structure with thickness of 0.4 $\mu m$.

## 4. Conclusion

In this work, we derive the existence of non-diagonal elements of $\chi^{(1)}$ tensor in domain walls according to previous study about mirror symmetry reduction of domain walls. At the condition of the existing of the new nonzero elements, we theoretically verify the emitting light is LCR according to the coupled wave equation. Such discontinuous distribution of non-diagonal elements of linear susceptibility tensor leads to the LCR phenomenon. Then, we experimentally demonstrate the LCR generation in ferroelectric domain walls and analyze the modulation effect of domain walls.

## Funding

National Natural Science Foundation of China (11734011, 61235009); National Key R&D Program of China (2017YFA0303700).